analytical chemistry

Article

Cite This: Anal. Chem. 2019, 91, 5184−5190

pubs.acs.org/ac

Online Measurement of Glucose Consumption from HepG2 Cells Using an Integrated Bioreactor and Enzymatic Assay

Anna G. Adams,[†] Radha Krishna Murthy Bulusu,[‡] Nikita Mukhitov,[†,§] Jose L. Mendoza-Cortes,[‡,∥] and Michael G. Roper*[,†]

[†]Department of Chemistry and Biochemistry, Florida State University, 95 Chieftain Way, Tallahassee, Florida 32306, United States

[‡]Department of Chemical and Biomedical Engineering, FAMU-FSU College of Engineering, 2525 Pottsdamer Street, Tallahassee, Florida 32310, United States

[∥]Department of Physics, Scientific Computing, Materials Science and Engineering, High Performance Materials Institute, and Condensed Matter Theory, National High Magnetic Field Laboratory (NHMFL), Florida State University, 1800 Paul Dirac Drive, Tallahassee, Florida 32310, United States

Supporting Information

ABSTRACT: Hepatocytes help to maintain glucose homeostasis in response to a variety of signals, including pancreatic hormones such as insulin. Insulin is released from the pancreas with variable dynamics, yet the role that these play in regulating glucose metabolism in the liver is still unclear. In this study, a modular microfluidic system was developed to quantitatively measure the effect of insulin dynamics on glucose consumption by a human hepatocarcinoma cell line, HepG2. A microfluidic bioreactor that contained 10^6 HepG2 cells was cultured for up to 10 days in an incubator. For glucose consumption experiments, the bioreactor was removed from the incubator and connected with reagents for an enzymatic glucose assay. The mixed components were then delivered into a droplet-based microfluidic system where the intensity of the fluorescent product of the enzyme assay was used to quantify the glucose concentration. By optimizing the mixing time of the reagents, the dynamic range of the enzymatic assay was adjusted to 0−12 mM glucose and had a time resolution of 96 ± 12 s. The system was used to observe rapid changes in insulin-induced glucose consumption from HepG2 cells. This assay format is versatile and can be expanded to measure a variety of hepatic metabolites, such as lactate, pyruvate, or ketone bodies, which will enable the correlation of pancreatic hormone dynamics to liver metabolism.

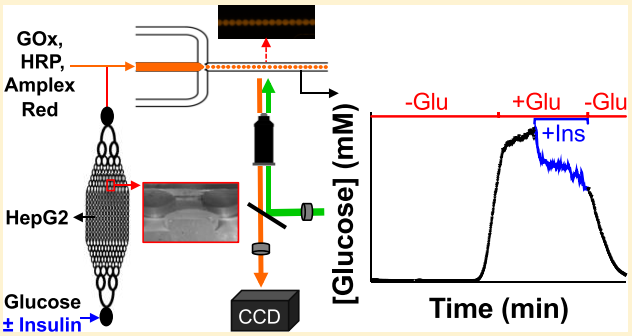

Worldwide, 425 million people have diabetes, with numbers continuing to increase every year.[1] Of those individuals, 90% have type II diabetes, which is a result of defective insulin secretion from the pancreas and insulin resistance in peripheral tissues, ultimately leading to abnormal glucose levels in the blood. The pancreas and liver are two organs that help maintain euglycemia. When blood glucose levels are too high or too low, the pancreas releases insulin and glucagon to stimulate anabolic and catabolic processes, respectively, in the liver and other organs. This interorgan signaling is essential for maintaining blood glucose levels around 5 mM.

Hepatocytes make up 70−85% of the liver, and help control glucose levels by converting excess glucose to glycogen for storage (glycogenesis), breaking down glycogen to replenish glucose levels (glycogenolysis), generating glucose via precursors (gluconeogenesis), and converting lactate to glucose in the Cori cycle.[2] Appropriate metabolic flux through these pathways is necessary to maintain homeostasis, and its disruption can have detrimental effects on overall glucose metabolism.

While the effects of insulin and glucagon on whole body glucose levels have been known for decades, how the dynamic release profiles of these peptides consisting of rapid changes in their levels, including oscillations with periods from 3 to 15 min, affects hepatic metabolism has only been sparsely investigated. To investigate these effects, it would be ideal to have an in vitro system that enables automated perfusion of pancreatic hormones to hepatocytes coupled with real-time detection of metabolic output. The use of in vitro hepatocyte systems for toxicology, pharmacology, and metabolism studies have become popular recently as they allow a mimic of the microstructure, properties, and metabolic functions of the liver.[3−16] There are several examples of hepatocyte-filled microfluidic devices that have incorporated sensors for measuring various components of metabolism and function during long-term culture. Some examples of monitored

Received: December 17, 2018
Accepted: March 19, 2019
Published: March 19, 2019

DOI: 10.1021/acs.analchem.8b05798
Anal. Chem. 2019, 91, 5184−5190

analytes include oxygen,[4] albumin and transferrin release,[5] and glucose uptake and lactate production.[6] However, these measurements have not been applied to examine the effects of pancreatic hormone dynamics.

In this work, we developed a microfluidic bioreactor for optimizing growth and maintaining structure and function of HepG2, a human hepatocarcinoma cell line. This microfluidic bioreactor successfully enabled culture of HepG2 for up to 10 days in a cell culture incubator. When desired, the device could be removed and the extracellular output from the bioreactor combined with enzymatic glucose reagents. The combined solutions were encapsulated into a droplet-based microfluidic system and the intensity of the resulting fluorescent assay product in the droplets was measured. The incubation time of the assay was optimized for measurement of glucose from 0–12 mM, the typical range of extracellular glucose concentrations. This system allowed the effect of insulin on glucose consumption in the HepG2 cells to be observed and quantified online and in near real-time. Additionally, the perfusion and detection systems are versatile and can be expanded to deliver various dynamic hormone perfusion profiles and measure a variety of different metabolic products using different assay reagents.

EXPERIMENTAL SECTION

Chemicals and Reagents. Cosmic calf serum (CCS) was obtained from Hyclone Laboratories (South Logan, UT). Gentamicin was from Lonza (Wakersville, MD). The 100× antibiotic–antimycotic (Ab/Am) and TrypLE were from Life Technologies (Gaithersburg, MD). Eagle's Minimum Essential Medium (EMEM) and Leibovitz's L-15 medium were purchased from the American Type Culture Collection (ATCC) (Manassas, VA). Matrigel and mineral oil were obtained from VWR International (Radnor, PA). Polydimethylsiloxane (PDMS) prepolymer (Sylgard 184) was from Dow Corning (Midland, MI). All solutions were prepared using ultrapure DI water (NANOpure Diamond System, Barnstead International, Dubuque, IA) and filtered using 0.2 μm nylon syringe filters (Pall Corporation, Port Washington, NY). All other reagents were purchased from Sigma-Aldrich (St. Louis, MO) unless stated otherwise.

Microfluidic Bioreactor Fabrication. The microfluidic bioreactor was based on a previous design[7] and fabricated using conventional soft lithography from PDMS at a 10:1 ratio of base to curing agent. The design contained two layers; all channels and structures in both layers were 100 μm in height and the dimensions were verified using a portable surface roughness tester (SJ-310 Series, Mitutoyo, Aurora, IL). The access holes were fabricated using a titanium nitride hole punch (SYNEO, Angleton, TX) and were 1.65 mm in diameter.

HepG2 Culture and Characterization. The human hepatocarcinoma cell line, HepG2, was obtained from ATCC and cultured in T25 or T75 flasks in EMEM supplemented with 10% CCS, 1% Ab/Am, and 0.1% gentamicin.

To perform growth curve measurements, five PDMS bioreactors were precoated with 60 μL of 3 mg mL^{-1} Matrigel for 1 h followed by a rinse with serum-free EMEM. After coating, 60 μL of HepG2 cells (1.6×10^3 μL^{-1}) were loaded into the bioreactor and incubated at 37 °C with 5% CO_2 for 24 h. A syringe pump was then used to deliver supplemented EMEM at a flow rate of 5 μL min^{-1} over 10 days with the outlet of the device connected to Tygon tubing (0.02" ID × 0.060" OD, Cole-Parmer North America, Vernon Hills, IL) and directed to a waste vial. Every other day, one bioreactor was removed from the incubator and TrypLE was added to the device and incubated for 5 min at 37 °C to detach the HepG2 cells. The released cells were counted and assessed for viability with a Cedex HiRes Analyzer (Roche Custom Biotech, Indianapolis, IN). To determine the metabolic activity of HepG2 cells cultured in the device, 100 μL of extracellular output was sampled daily and stored in a −80 °C freezer until analysis. The amounts of albumin (BioVision, Milpitas, CA) and urea (Cayman Chemical, Ann Arbor MI) in the samples were determined using standard kits. To compare growth and function in the bioreactors to 2D cultures, HepG2 were cultured for 10 days in T25 flasks with extracellular samples collected every day for similar assays. Growth curves and measurements of albumin and urea were conducted in triplicate.

Automated Perfusion. To ensure consistent numbers of cells for online glucose measurements, cell cultures from T75 flasks were diluted with an appropriate volume of supplemented EMEM to 1.6×10^4 HepG2 μL^{-1}, and 60 μL were added to each bioreactor. These cells were incubated overnight with no flow to allow the cells to attach. The bioreactor was then attached to an automated pressure-driven flow system (OB1Mk3, Elveflow, Paris, France) for perfusion with glucose and insulin. Two different solutions could be delivered to the bioreactor; the solutions were composed of Leibovitz's L-15 Media, which was supplemented with the concentrations of glucose or insulin given in the text. The total flow rate to the bioreactor was maintained at 5 μL min^{-1}, while the flow rates from the two input solutions were adjusted to achieve the desired concentration of glucose or insulin. The flow rates were monitored using inline flow sensors (MFS3, Elveflow).

The bioreactor was placed on a custom rectangular copper plate that had four Peltier devices (20.0 × 40.0 × 4.3 mm, Custom Thermoelectric, Bishopville, MD) on each side of the plate. The temperature of the copper plate was controlled using an Accuthermo FTC-100D controller (Freemont, CA) in conjunction with a J-type thermocouple (SA1-J, Omega Engineering Inc., Samford, CT) attached to the center of the copper block. The temperature of the plate was adjusted so that the temperature inside the bioreactor was 37 °C as measured using a flexible wire microthermocouple (IT-18, Physitemp Instruments, Inc., Clifton, NJ). The entire setup consisting of the microfluidic device, copper plate, thermocouple, and Peltiers were housed in a home-built 3D-printed holder.

The output of the bioreactor was directed out of the 3D-printed holder and into a three-way microfluidic connector (P-512, IDEX Health and Science, Oak Harbor, WA) via Tygon tubing. The other input to the three-way connector consisted of a solution containing the glucose assay reagents, made up of 1.9 mL of a 50 mM phosphate buffered solution (pH 7.4), 0.04 mL of 10 U mL^{-1} horseradish peroxidase (HRP), 0.04 mL of 100 U mL^{-1} glucose oxidase (GOx), and 0.02 mL of 10 mM Amplex Red. These reagents were in a third reservoir with their flow rate (5 μL min^{-1}) also controlled by the pressure driven flow system with an inline flow sensor. The output of the three-way connector was delivered via Tygon tubing to a hydrophobic flow-focusing microfluidic device (190 μm etch depth, Dolomite Microfluidics, Royston, U.K.) as the dispersed phase. The continuous phase, mineral oil with 1% Span 80, was

DOI: 10.1021/acs.analchem.8b05798
Anal. Chem. 2019, 91, 5184–5190

delivered to the flow-focusing droplet device via a syringe pump at a flow rate of 15 μL min^{-1}.

Following each experiment, bioreactors were removed from the experimental setup, returned to the incubator, and reconnected to syringes via Tygon tubing, where hepatocytes were continuously perfused with fresh media.

Optical Detection System. The droplet junction device was placed on the stage of a Nikon Eclipse Ti−S inverted microscope (Nikon Instruments Inc., Melville, NY). For imaging the fluorescence in droplets, a Xenon arc lamp (Lambda XL, Sutter Instruments, Novato, CA) with a 535 ± 15 nm excitation filter was used as the excitation source and made incident on a 565 nm dichroic mirror (Omega Optical, Inc., Brattleboro, VT). The excitation light was focused into the droplet microfluidic device using a 2×, 0.06 NA objective (Nikon Instruments, Inc.). Emission light was collected with the same objective, passed through the dichroic filter, a 595 ± 30 nm emission filter (Omega Optical), and detected with a CCD camera (Photometrics, Tucson, AZ). Fluorescence images were acquired with a 42 ms exposure every 5 s. The timing of the images and the lamp shutter were controlled by Nikon NIS Elements software (Nikon Instruments, Inc.). With the estimated rate of droplet production, the image captured with a 42 ms exposure consisted of ∼18 droplets. The average fluorescence intensity of the image was measured using a region of interest set in the Nikon NIS Elements software.

Modeling of Fluid Dynamics. The velocity, pressure, and shear stress in the bioreactor were modeled using COMSOL Multiphysics 5.3 (COMSOL, Inc., Burlington, MA). Simulation parameters assumed water was flowing through the device using an inlet velocity of 0.00014 m s^{-1} and an inlet concentration of 1 mol m^{-3}, at room temperature. Laminar flow and transport in dilute species were considered in the physics of the model with zero velocity (no-slip condition) and zero flux at the walls.

Data Analysis. Unless otherwise noted, all figures are shown with the timing of the extracellular glucose delivery in red bars above the traces and timing of insulin delivery with blue bars. Results are presented as averages with error bars corresponding to ±1 standard error of the mean (SEM) or standard deviation (SD) as noted in the text. All statistical analyses were performed using unpaired 1-tailed t tests.

RESULTS AND DISCUSSION

In this work, we demonstrate an optical detection system for online measurement of rapid changes in glucose output from HepG2 in response to pancreatic hormone perfusion. With this system, the HepG2 could be cultured for up to 10 days in a conventional incubator in one microfluidic system and, when desired, connected to a separate microfluidic system for determination of extracellular glucose levels. In response to an increase in insulin, increases in glucose consumption were observed that reduced the extracellular glucose level that was measured.

Microfluidic System for Culturing HepG2. The bottom layer of the microfluidic bioreactor contained a 1 cm^2 area with 100 μm tall pillars and structures to facilitate growth of HepG2 cells in three dimensions. To minimize shear stress on the cells, the ceiling of the cell culture area was extended 100 μm above the pillars. The design of the bioreactor is provided in more detail in the Supporting Information (SI), including Figure S-1. To characterize the flow in the device, a finite element simulation was used to visualize the pressure and velocity profiles without cells when the input flow rate was set at 5 μL min^{-1} (Figure S-2A−C). As expected, the pressure decreased linearly across the device and the highest linear velocities were found at the inlet and outlet. However, the velocity in the cell region was substantially lower due to the larger cross-sectional area of this region. This design reduced the calculated shear stress to <10 mPa in the cell culture area (Figure S-2D,E), lower than other devices that have been used for maintaining HepG2 in culture.[8−11]

Once the design was fixed, HepG2 cells were loaded into the device and cultured in flowing media in a CO_2 incubator for up to 10 days. The cells in the bioreactor showed higher albumin and urea release compared to 2D cultures, growth curves that exhibited all phases of cell growth, and >90% viability for over a week (Figure S-3). These results parallel other reports of HepG2 cell systems in 3D culture.[12−16]

Incorporation of Online Glucose Assay. For determination of extracellular glucose levels, the bioreactor was removed from the incubator and attached to glucose assay reagents and a droplet generating microfluidic system, as shown in Figure 1A. Two solutions containing 0 mM glucose, and either 10 mM glucose or 10 mM glucose with 200 nM insulin were input into the bioreactor using a pressure-driven flow system. The flow rate into the bioreactor was held

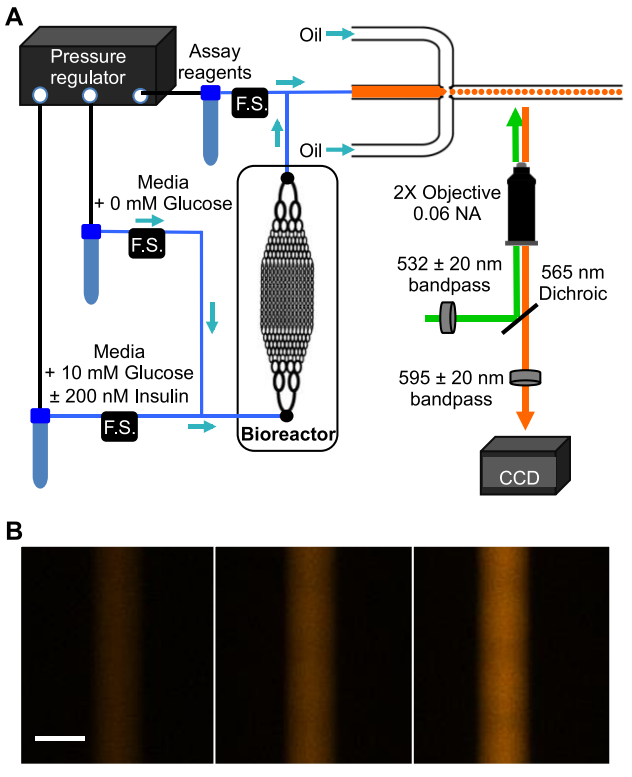

Figure 1. Setup for automated perfusion of HepG2 with online glucose monitoring. (A) A pressure-driven flow system was used to deliver media containing different concentrations of glucose and insulin to the input of the bioreactor. Flow sensors (F.S.) were used to maintain accurate flow rates of the reagents. The output of the bioreactor mixed with enzymatic glucose assay reagents for 54 s before entering a flow-focusing device that generated droplets. (B) A zoomed-in region is shown from three fluorescence images of the channel containing the droplets during a 42 ms exposure. From left to right, the final glucose concentration was 2.4, 7.2, and 12 mM. The scale bar is 390 μm.

DOI: 10.1021/acs.analchem.8b05798
Anal. Chem. 2019, 91, 5184−5190

constant at 5 μL min^{-1}, but the individual flow rates of the perfusion solutions were varied to produce different concentrations of the reagents. This was achieved by programming the perfusion system to modify the flow rate of the two input solutions independently. An example of the individual flow rate profiles of all solutions can be seen in Figure S-4. In addition, more complicated profiles could be produced by switching out the idle reservoir during the experiment, while flow was being delivered from the active reservoir. In this way, concentrations of glucose, insulin, and combinations of the two reagents could be varied in time as dictated by the experiment, while the total flow rate of the solution to the bioreactor remained constant. All flow control occurred upstream of the detection system and, therefore, did not influence the analysis of the extracellular glucose level.

The perfusate exited the bioreactor and mixed 1:1 with the reagents for measurement of extracellular glucose. These reagents consisted of a commercially available coupled enzymatic assay using GOx, HRP, and Amplex Red.[17] Amplex Red based assays have been successfully incorporated into the output of other cell-based microfluidic devices. For example, assays for glycerol and fatty acid production from adipocytes were made online with limits of detection in the low micromolar regime.[18,19] The biggest challenge for incorporation of this commercial assay into our online system was signal saturation due to the high concentrations of glucose that were being perfused in the bioreactor (0−12 mM) compared to the concentrations that were intended for the assay (0−100 μM). To enable detection of these higher glucose concentrations, the resorufin fluorescence was measured shortly after mixing the enzymatic reagents with the bioreactor perfusate. Using the recommended ratio of reagents, they were delivered at a 1:1 flow rate ratio with the bioreactor output into a mixing tee and then delivered to a flow-focusing device as the dispersed phase. The length of the tubing from the mixing tee into the flow-focusing device was chosen such that there would be just enough time to fully mix the perfusate with the glucose assay reagents (calculated travel time of 54 s vs a calculated mixing time of 49 s), ensuring a homogeneous solution entered the flow-focusing device, but without excessive incubation.

Detection in the droplets was made 5 mm downstream of the droplet production intersection, which only allowed ∼684 ms for mixing within the droplets. This total mixing time of less than 55 s was well below the recommended 30 min incubation time for the lower concentrations of glucose and allowed the use of extracellular glucose concentrations from 0−12 mM.

The droplets were imaged every 5 s using a 2× objective and a CCD camera for detection with a 42 ms exposure. As can be seen in Figure 1B, at this exposure time and droplet production rate, the individual droplets could not be resolved. Nevertheless, using regions of interest to define the background and the entire length of the droplet channel, the background-subtracted fluorescence from each image was calculated and recorded, resulting in a data point every 5 s. We estimate that the fluorescence was measured from 18 droplets during the 42 ms exposure (see SI and Figure S5 for information on this estimate). The droplet size was measured to be 288 ± 7 μm (average ± SD, n = 51 droplets).

An example from a calibration of the glucose measurement is shown in Figure 2 where glucose levels were changed in time and delivered through an unfilled bioreactor into the glucose detection system. The glucose levels that were delivered to the bioreactor are shown by the red line and correspond to the right y-axis, while the background-subtracted fluorescence intensities of the droplets, as described above, are shown by the black data points and corresponds to the left y-axis. The intensities during the middle 5 min (n = ∼60 data points) at each glucose concentration were averaged and are shown by the open gray circles and the error bars shown are ±1 SD. A linear response of the average resorufin fluorescence to the glucose concentration was observed ($y = 255x + 66$, $r^2 = 0.99$). The calculated limit of quantitation and limit of detection were 0.7 and 0.2 mM, respectively. The response time measured across each of the calibration solutions, a zoomed in portion of which is shown in the inset of Figure 2, was 96 ± 12 s (average ± SD, n = 9 measurements), indicating that rapid changes in extracellular glucose could be measured.

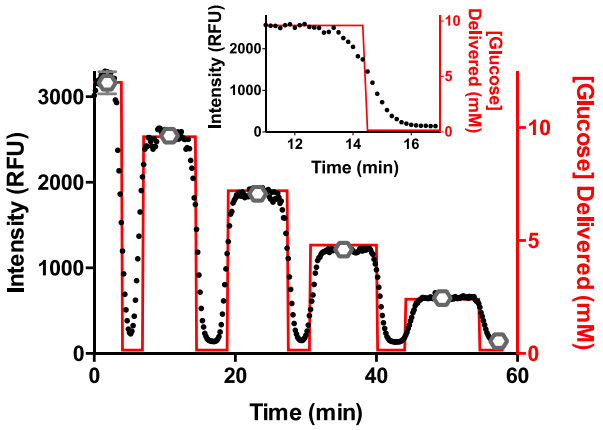

Figure 2. Online glucose assay calibration. The calibration of resorufin fluorescence to glucose concentrations from 0−12 mM is shown. The black data points are the background-subtracted resorufin intensity values taken every 5 s from 18 droplets and correspond to the left y-axis. The red line represents the known glucose concentration that was delivered to the perfusion system. The average resorufin intensity at each glucose plateau is shown by the open gray circles with ±1 SD shown by the error bars. The inset is a zoomed-in portion of the shaded region highlighting the response time from one calibration solution.

To ensure that the assay was not influenced by extracellular insulin, an unfilled chip was perfused with 12 mM glucose for 30 min, followed by 12 mM glucose with 200 nM insulin. This alternating perfusion with insulin was repeated at 6 and 0 mM glucose and the data and calibration is shown in Figure S-6. No difference in resorufin fluorescence was observed in the presence of insulin. Daily calibration curves were obtained at three glucose levels.

Application of Insulin Perfusion to HepG2. To determine if the newly developed assay could be used for in vitro measurements, initial experiments were designed to measure the glucose consumption rates in the absence and presence of insulin. To perform these assays, the bioreactor was taken out of the CO_2 incubator, coupled with the glucose assay reagents, and connected to the droplet-generating device for measurement of extracellular glucose levels. Following connection, the bioreactor was perfused at 0 mM glucose to deplete extracellular glucose and glycogen stores. This time is seen in Figure 3A by the initial decrease in measured glucose to <1 mM. After 30 min, hepatocytes were given a combination of 200 nM insulin in 10 mM glucose, which resulted in the increase in measured glucose that can be readily

DOI: 10.1021/acs.analchem.8b05798
Anal. Chem. 2019, 91, 5184−5190

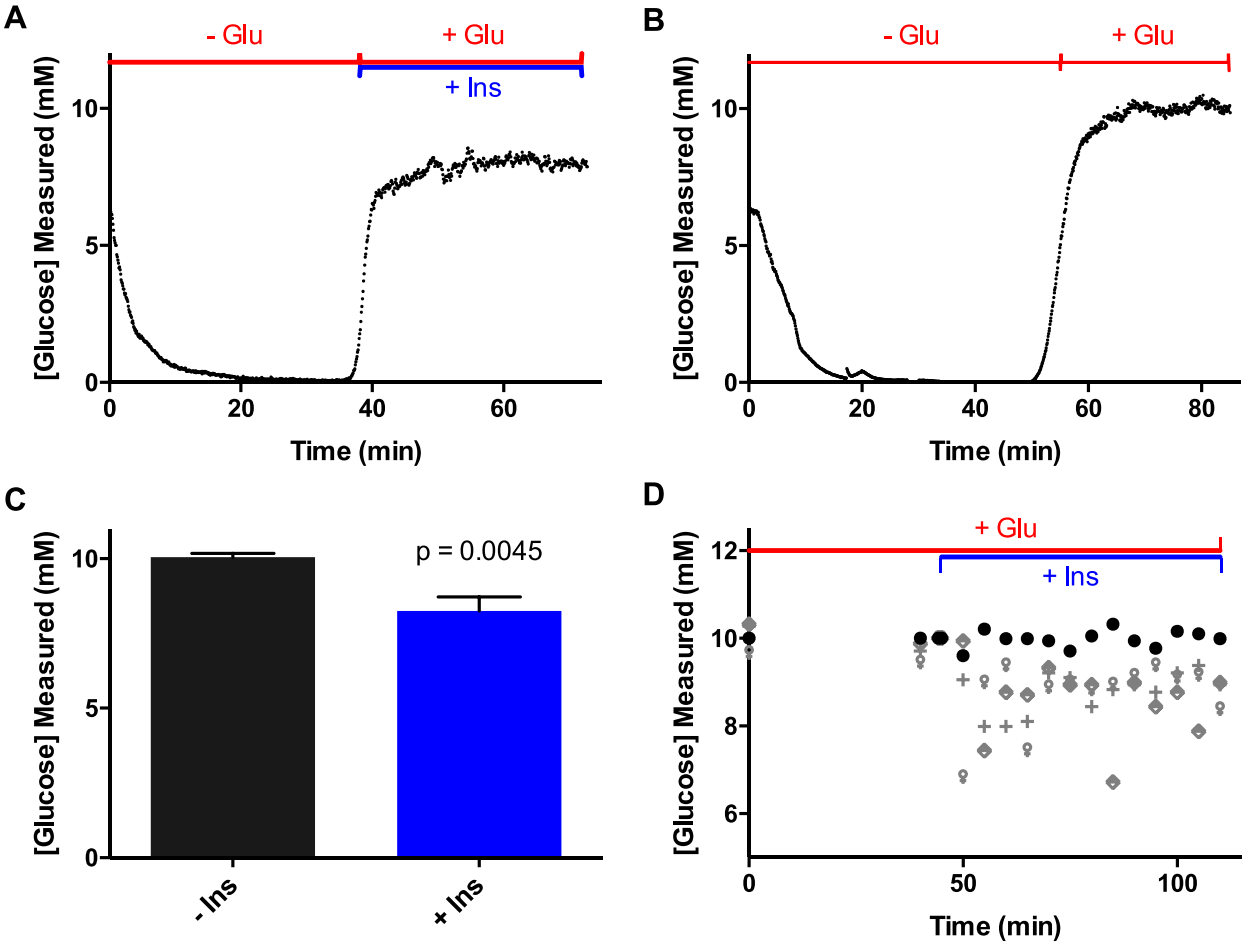

Figure 3. Glucose output following perfusion with and without 200 nM insulin. (A) Approximately 10^6 HepG2 were perfused with 0 mM glucose followed by 10 mM glucose with 200 nM insulin. (B) In this experiment, ~10^6 HepG2 were initially perfused with 0 mM glucose followed by 10 mM glucose only. (C) The average measured glucose concentration from eight perfusion experiments, four with 10 mM glucose with (+Ins) and four without (−Ins) 200 nM insulin. Error bars correspond to ±1 SEM from the four trials. The *p*-value corresponds to an unpaired one-tailed *t* test. (D) Four bioreactors filled with ~10^6 HepG2 were perfused with 10 mM glucose for 45 min. After this time, one of the bioreactors continued to be perfused with 10 mM glucose (circles), while the others were perfused with 10 mM glucose with 100 nM insulin. The measured glucose level at each time point for the four bioreactors are shown. For this experiment, the glucose concentration was measured using a standard glucose meter every 5 min.

seen in Figure 3A. The glucose level during this experiment was 7.9 ± 0.3 mM (average ± SD, n = 359 data points). This experiment was repeated an additional three times with separate devices, resulting in a glucose output during the delivery of glucose and insulin of 8.3 ± 0.5 mM (average ± SEM, n = 4 trials). The traces from the three additional experiments are shown in Figure S-7 and Table S-1 details the average glucose level for all experiments. This average glucose level resulted in a calculated consumption rate of 37 μg glucose h^{-1} 10^6 $cells^{-1}$, which is similar to other rates reported for HepG2 cells.[6,20]

Control experiments were performed by delivering 0 mM glucose media to four bioreactors containing a similar number of cells as that described above, followed by perfusion with 10 mM glucose without insulin. A representative trace is shown in Figure 3B, which showed a glucose level of 9.9 ± 0.3 mM (average ± SD, n = 360 points). The glucose output from the four control experiments during the delivery of glucose was 10.1 ± 0.1 mM (average ± SEM, n = 4 trials). The traces from the three additional control experiments are shown in Figure S-8 and detailed in Table S-1. Since the measured extracellular glucose level was similar to that being delivered, a glucose consumption rate could not be calculated in the absence of insulin.

As seen in Figures S-7 and S-8, there was some variability in the timing of reagent delivery between experiments that were due to small particulates or bubbles introduced from one of the solution reservoirs (seen as a rapid increase in pressure in the flow system). When this occurred, the tubing would be disconnected to clear it out and resulted in slight differences in the times glucose or insulin was delivered. These clogs typically occurred when new reservoirs were attached, therefore, flow to the bioreactor did not have to be stopped during purging. This timing variability does not allow for the data traces to be overlapped to show an average trace; however, one of the benefits of the system is the observation of the glucose changes in real time regardless of the timings. Also, the glucose consumption values reported are normalized to the time that the insulin was delivered.

Nevertheless, the average glucose level that was measured during insulin delivery in four experiments was lower than the average glucose level that was measured without insulin (p = 0.0045, unpaired one-tailed t test, Figure 3C).

DOI: 10.1021/acs.analchem.8b05798
Anal. Chem. 2019, 91, 5184−5190

To compare these online experiments to more conventional methods of glucose measurement, a hand-held glucose meter was used to measure glucose efflux from the bioreactor. Hepatocytes in four bioreactors were perfused with 10 mM glucose for 45 min. After this period, three of the bioreactors were perfused with 10 mM glucose with 100 nM insulin and one bioreactor continued receiving only 10 mM glucose. Measurements of glucose output were taken every 5 min with a hand-held glucose meter (Freestyle Lite, Abbott Laboratories, Abbott Park, IL). Similar to the online glucose assay, there was a decrease in the measured glucose concentration in the three bioreactors after the addition of insulin. The glucose level during the insulin delivery at each time point from the three bioreactors are shown by the different symbols in Figure 3D. The glucose level across all time points during insulin delivery was 8.9 ± 0.1 mM (average ± SEM, n = 3 trials), while the glucose concentration during the same time points from the control bioreactor was 9.9 ± 0.2 mM (average ± SD, n = 15 data points; Figure 3D, circles). The similar results obtained using a conventional method of glucose measurement gave us confidence that the online system was working as intended and could be used for examining rapid changes in the glucose levels.

Rapid Changes in Glucose Levels. To examine dynamic changes in glucose levels, another set of experiments was performed where insulin was added in the middle of the glucose perfusion. As shown in Figure 4A, perfusion with 0 mM glucose media reduced the measured extracellular glucose level to ∼0 mM. This was followed by 10 mM glucose perfusion for 15 min, resulting in a measured extracellular glucose level close to the expected 10 mM. After this time, 200 nM insulin in 10 mM glucose was delivered for 20 min, producing an abrupt decrease in the extracellular glucose level. This experiment was repeated three times with all traces shown in Figure S-9 and described in Table S-1. The glucose level measured during insulin perfusion was 8.7 ± 0.6 mM (average ± SEM, n = 4 trials), significantly lower than the glucose level during perfusion without insulin, 10.1 mM ± 0.1 (average ± SEM, n = 4 trials, p = 0.023, unpaired one-tailed t test).

To ensure the effects we observed were not due to an experimental artifact, another set of experiments was performed where insulin was removed during high glucose perfusion. In these experiments, two bioreactors were first perfused with 0 mM glucose for 50 min, followed by perfusion with 200 nM insulin in 10 mM glucose, with one of the experiments shown in Figure 4B. The glucose level during perfusion was 8.9 ± 0.7 mM (average ± SEM, n = 2 trials, Table S-1). After this time, the perfusion was changed to 10 mM glucose without insulin, which resulted in an increase in the measured glucose output (10.0 ± 0.3 mM, average ± SEM, n = 2 trials). While the measured glucose levels during perfusion with and without insulin in these experiments were not significantly different (p = 0.089), the small number of replicates may have been a factor in the lack of significance.

CONCLUSION

In this work, a method for online measurement of glucose from cultured hepatocytes was developed using an optical detection system. The calibration of millimolar concentrations of glucose using a coupled enzymatic reaction was made possible by measurement before the reaction went to completion. Although other in vitro hepatocyte systems have incorporated methods for measuring various components of metabolism and

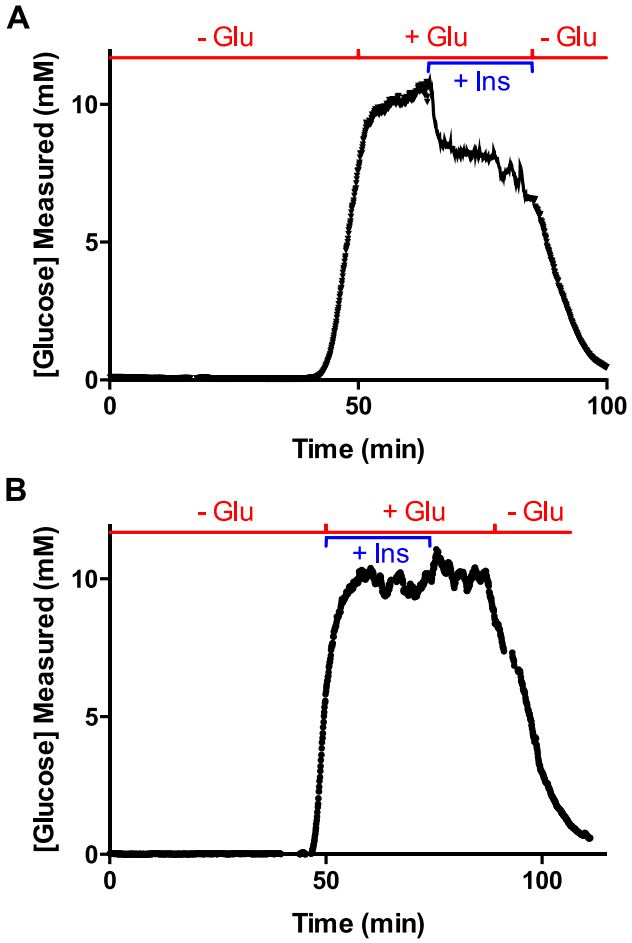

Figure 4. Rapid changes in glucose consumption. (A) Glycogen was depleted from HepG2 by initial perfusion with 0 mM glucose. The extracellular glucose was then increased to 10 mM for 35 min with insulin delivered during the last 20 min. Glucose was then decreased to 0 mM until the end of the experiment. (B) The measured extracellular glucose concentration is shown for HepG2 perfused with an initial 0 mM glucose followed by 200 nM insulin in 10 mM glucose. Insulin was then removed, and 10 mM glucose was delivered without insulin for 15 min followed by perfusion with 0 mM glucose to the end of the experiment.

function during long-term culture,[3−16] the system described here is significant and innovative in that it is suitable to examine acute and rapid changes of extracellular glucose, which will enable the effects of dynamic pancreatic hormone stimulations to be examined. Use of the online system was not only advantageous for reproducible timing of the glucose measurements, but the format also allowed the culture of the cells to be performed under independent conditions. This modular approach to cell culture and online measurements could be beneficial in coupling other in vitro devices to one another or to other measurement systems, and it could be possible to examine the role of shear stress on hepatocyte behavior. Although glucose was measured in this study, various metabolites involved in hepatic glucose metabolism such as lactate, pyruvate, or ketone bodies, can be incorporated into similar online assays. Additionally, the versatility of the automated perfusion system will allow for more complicated, in vivo-like hormonal profiles to be delivered to the cells to test their effect on glucose metabolism directly. This methodology has the potential to shed light on glucose level management in

DOI: 10.1021/acs.analchem.8b05798
Anal. Chem. 2019, 91, 5184−5190

prediabetes and type II diabetes, as well as provide insight into proper glucose regulation within the body. We expect that this system will enable the observation of hepatocyte dynamics in response to more complicated pancreatic hormone profiles like those observed in vivo in future work.

■ ASSOCIATED CONTENT

Supporting Information

The Supporting Information is available free of charge on the ACS Publications website at DOI: 10.1021/acs.analchem.8b05798.

Detailed measurements and images of bioreactor; Metabolic characterization of HepG2; finite element analyses of pressure, velocity, and shear stress; additional data traces of cell experiments; validation of data unaffected by external factors (PDF)

■ AUTHOR INFORMATION

Corresponding Author

*Phone: 850-644-1846. Fax: 850-644-8281. E-mail: roper@chem.fsu.edu.

ORCID

Michael G. Roper: 0000-0002-0184-1333

Present Address

§Department of Biological Engineering, Massachusetts Institute of Technology, Cambridge, Massachusetts, 02139, United States.

Author Contributions

The manuscript was written through contributions of all authors. All authors have given approval to the final version of the manuscript.

Notes

The authors declare no competing financial interest.

■ ACKNOWLEDGMENTS

The help of G. Ryan Adams is gratefully acknowledged for acquiring the scanning electron microscopy images of the bioreactor. This work was supported by a grant from the National Institutes of Health (R01 DK080714). J.L.M.-C. acknowledges startup funds from the Energy and Materials Initiative at Florida State University. A portion of this work was performed at the National High Magnetic Field Laboratory, which is supported by National Science Foundation Cooperative Agreement No. DMR-1644779 and the State of Florida.

■ REFERENCES

(1) International Diabetes Federation. Idf Diabetes Atlas. In *IDF Diabetes Atlas*; Karuranga, S., Fernandes, J. da R., Huang, Y., Malanda, B., Eds.; International Diabetes Federation, 2015; pp 1−527.

(2) Moore, M. C.; Coate, K. C.; Winnick, J. J.; An, Z.; Cherrington, A. D. *Adv. Nutr.* **2012**, *3* (3), 286−294.

(3) Huh, D.; Hamilton, G. A.; Ingber, D. E. *Trends Cell Biol.* **2011**, *21*, 745−754.

(4) Prill, S.; Bavli, D.; Levy, G.; Ezra, E.; Schmälzlin, E.; Jaeger, M. S.; Schwarz, M.; Duschl, C.; Cohen, M.; Nahmias, Y. *Arch. Toxicol.* **2016**, *90* (5), 1181−1191.

(5) Riahi, R.; Shaegh, S. A. M.; Ghaderi, M.; Zhang, Y. S.; Shin, S. R.; Aleman, J.; Massa, S.; Kim, D.; Dokmeci, M. R.; Khademhosseini, A. *Sci. Rep.* **2016**, *6*, 24598.

(6) Bavli, D.; Prill, S.; Ezra, E.; Levy, G.; Cohen, M.; Vinken, M.; Vanfleteren, J.; Jaeger, M.; Nahmias, Y. *Proc. Natl. Acad. Sci. U. S. A.* **2016**, *113* (16), E2231−E2240.

(7) Leclerc, E.; Sakai, Y.; Fujii, T. *Biomed. Microdevices* **2003**, *5* (2), 109−114.

(8) Tanaka, Y.; Yamato, M.; Okano, T.; Kitamori, T.; Sato, K. *Meas. Sci. Technol.* **2006**, *17* (12), 3167−3170.

(9) Pereira Rodrigues, N.; Sakai, Y.; Fujii, T. *Sens. Actuators, B* **2008**, *132*, 608−613.

(10) Leclerc, E.; El Kirat, K.; Griscom, L. *Biomed. Microdevices* **2008**, *10* (2), 169−177.

(11) Esch, M. B.; Mahler, G. J.; Stokol, T.; Shuler, M. L. *Lab Chip* **2014**, *14* (16), 3081−3092.

(12) Ramaiahgari, S. C.; Den Braver, M. W.; Herpers, B.; Terpstra, V.; Commandeur, J. N. M.; Van De Water, B.; Price, L. S. *Arch. Toxicol.* **2014**, *88* (5), 1083−1095.

(13) Sakai, Y.; Naruse, K.; Nagashima, I.; Muto, T.; Suzuki, M. *Cell Transplant* **1999**, *8* (5), 531−541.

(14) Dubiak-Szepietowska, M.; Karczmarczyk, A.; Jönsson-Niedziólka, M.; Winckler, T.; Feller, K. H. *Toxicol. Appl. Pharmacol.* **2016**, *294*, 78−85.

(15) Davidson, M. D.; Lehrer, M.; Khetani, S. R. *Tissue Eng., Part C* **2015**, *21* (7), 716−725.

(16) Jang, M.; Neuzil, P.; Volk, T.; Manz, A.; Kleber, A. *Biomicrofluidics* **2015**, *9* (3), 034113.

(17) Zhou, M.; Diwu, Z.; Panchuk-Voloshina, N.; Haugland, R. P. *Anal. Biochem.* **1997**, *253* (2), 162−168.

(18) Clark, A. M.; Sousa, K. M.; Jennings, C.; MacDougald, O. A.; Kennedy, R. T. *Anal. Chem.* **2009**, *81* (6), 2350−2356.

(19) Dugan, C. E.; Cawthorn, W. P.; MacDougald, O. A.; Kennedy, R. T. *Anal. Bioanal. Chem.* **2014**, *406* (20), 4851−4859.

(20) Baudoin, R.; Griscom, L.; Prot, J. M.; Legallais, C.; Leclerc, E. *Biochem. Eng. J.* **2011**, *53* (2), 172−181.

DOI: 10.1021/acs.analchem.8b05798
Anal. Chem. 2019, 91, 5184−5190